

High Temperature Air oxidation of 22Cr 11-19Ni Steels

U. BERNABAI - Dipartimento ICMMPM, Università "La Sapienza" Roma, Italy, M. CAVALLINI - Dipartimento Ing. Industriale, Università di Cassino, Italy, F. FELLI - Dipartimento ICMMPM, Università "La Sapienza" Roma, Italy and A. TAMBA - Centro Sviluppo Materiali, Roma, Italy

Abstract

Three 22% Cr austenitic steels with different Ni, Mn, N, and Si content (UNS S30908, S30815, and 309 modified), and a 25% Cr (S31008) have been tested in air at elevated temperatures in order to evaluate their resistance to oxidation. Isothermal and cycling tests have been carried out and a temperature upper limit has been established for the two working conditions: as the temperature corresponding to a steady mass gain of 2 mg/cm². The temperature limits in isothermal experiments are: S30908 and S31008 ≤ 1000°C; S30815 and 309 modified < 1100°C. In cycling tests the limits appear to be as follows: S30908 < 850°C, S30815 ≤ 850°C, S31008 and 309 modified ≤ 900°C. Silicon and rare earths appear to substantially improve the resistance in isothermal conditions, while chromium content appears to control the behaviour in cycling tests.

Riassunto

Quattro acciai inossidabili austenitici contenenti 22-25% circa di Cromo e diversi tenori di Ni, Mn, N e Si (UNS S30908, S31008, S30815, 309 modificato) sono stati provati in aria ad elevate temperature per valutarne la resistenza alla ossidazione. Sono state eseguite prove isoterme e cicliche e per ogni condizione di lavoro sono stati stabiliti dei limiti superiori alle temperature di impiego in corrispondenza ad un acquisto di massa pari a 2 mg/cm². I limiti nelle prove isoterme sono: S30908 e S31008 ≤ 1000°C; S30815 e 309 modificato < 1100°C. Nelle prove cicliche i limiti sono invece: S30908 < 850°C, S30815 ≤ 850°C, S31008 e 309 modificato ≤ 900°C. Il silicio e le terre rare aumentano la resistenza alla ossidazione in condizioni isoterme, mentre è il cromo a controllare il comportamento in condizioni cicliche.

Introduction

Austenitic stainless steels such as AISI 321, AISI 309, AISI 310 are usually selected for high temperature services. These three types of steel are easily commercially available in different grades, as precisely reported in the Unified Numbering System (UNS) for metals and alloys. These grades differ mainly in terms of C and Si to match the great variety of practical industrial applications. These three families of heat resistant steels: 321, 309 and 310 offer different levels of resistance and reliability in terms of maximum temperature service, creep, mechanical properties at high temperature, capability to withstand environmental attack, long term metallurgical stability.

The three levels of reliability during high temperature service reflect mainly the set of properties offered by the base steel composition, namely 18Cr10NiTi (321), 22Cr13Ni (309) and 25Cr20Ni(310).

The intermediate alloying level of AISI 309 family covers quite satisfactorily the needs of a wide number of demanding high temperature applications in oxidant environment, thus resulting an acceptable compromise between cost and benefit.

Nevertheless a careful examination of the oxidation mechanisms and of the role of specific elements in improving resistance to high temperature scaling either in isothermal or cyclic situations can help to obtain better performances of 22Cr13Ni steels by proper minor alloying and composition balance.

Chromium-Nickel stainless steels designed for high-temperature service develop a protective scale mainly consistent in preferentially oxidized Cr₂O₃. Such an oxide must be as pure as possible; every contamination from either Fe or Mn produces less protective fast-growing spinels. At the outer gas/oxide interface the Fe⁺⁺ cation easily oxidizes to Fe⁺⁺⁺ allowing a fast oxygen ionisation. Iron oxide FeO is richer in cationic vacancies than NiO. Thus the kinetic control on oxidation of Fe Cr Ni alloys mainly consists in the control of Fe⁺⁺ flux toward the outer scale surface.

Silicon, a minor element always present in the composition of this grade of steels, is able to develop a beneficial action on the oxidation resistance [1]. No more spinels appear in 20 Cr - 25 Ni steels with silicon content higher than 0.9%. Bennett [2] found at the matrix/Cr₂O₃ oxide interface a continuous layer of amorphous SiO₂ with a 0.6% silicon content. Often, rather than a continuous layer (3-6 μm thick) globules or intrusions of Si-rich oxides develop. Lobb et al. [1], studying the influence of silicon on the oxidation at 900°C in CO₂ gas, found that 0.6% Si is needed for developing the minimum thickness of the

layer between Cr-oxide and metal. Higher Si contents allow higher layer thicknesses, not able to increase the oxidation control, and even susceptible to fail, thus breaking off the protectivity.

Manganese in the substrate appears to easily diffuse through the chromium oxide scale at the gas/oxide interface, where it forms a low-density MnCr_2O_4 spinel, susceptible to enhance compressive stresses during oxide growth and, thus, promoting spalling [3]. The silica (or silicates) layer, able to control the Fe^{++} ion, is less effective toward the Mn, whose content in the alloy composition must be contained at the lowest level, preferably under 0.8% [1].

As both Ni (expensive and not resistant in sulphurizing environments) and Mn contents must be reduced, carbon and nitrogen must be adopted as austenitizing elements.

The formation of a pure Cr_2O_3 scale needs favourable conditions, first of all an appropriate Cr content in the alloy, function of the oxidizing gas composition. N.Otsuka [4], studying Fe Cr Ni alloys oxidation at 600-900°C in water vapour, found that the continuous and compact Cr_2O_3 layer develops for Cr contents higher than 21%. Under the same composition, reduced grain size promotes an easier scale formation, as Cr diffusion in the metal occurs easily along the grain boundaries. In the same way cold working, enhancing reticular defects, promotes a more resistant scale.

Also rare earths, either as alloy elements or as dispersoids, enhance both the adhesion and the protectivity of the scale, particularly at the highest temperatures. The mechanism is suggested to consist in:

- a) an increased availability of nuclei for Cr_2O_3 formation,
- b) a better scale pegging,
- c) a modification in the mechanisms of Cr_2O_3 growth, which reduces the Cr^{+++} diffusion toward the outer surface and allows that of oxygen ions along the oxide grain boundaries.

A silicon content of 1% in Fe 26Cr alloys [5] promotes the formation of a protective Cr_2O_3 scale over near-surface nuclei of SiO_2 . Often a synergical action of Si and rare earths has been evidenced via the formation of oxides at the grain boundaries of the scale, able to stop the diffusion of different ions [6].

Both density and thermal expansion coefficients of the scale formed during oxidation on metallic surfaces are lower than matrix ones. Therefore oxide growth and temperature gradients cause stresses, failures and detachments. A crack in the scale gives an easy path for oxygen penetration; in case of spalling a virgin metallic surface, presumably with a reduced content of the protective elements already engaged in the formation of the former scale, is directly exposed to the oxidising elements. In the both cases the final result is an enhancement of scale growth. If spalling occurs a sudden mass loss is followed by a mass gain due to the formation of a new oxide, whose kinetic is the same of the initial stage of oxidation or else worse if a less protective oxide takes the place of the former.

Epitaxial compressive stresses appear usually during the first stages of oxidation. As the scale grows the stresses are less important. According to Stringer [7] the development of stresses during oxide growth causes plastic flow in the scale and creep in the substrate.

The continuous oxide formation inside the already formed scale, due to Cr and O ions migration, can produce buckling.

If the oxidation process occurs during thermal cycling, the thermal stresses and the thermo-mechanical properties of scale, metal and interface can deeply affect the performances of an alloy. Compressive, or else tensile stresses appear on the scale on cooling, according to the rate of the process from slow to shock. Every defect and discontinuity in scale and interface can promote cracks and detachments.

In order to promote a compact and adherent scale, the defect state at the metal/oxide matrix must be controlled. Voids accumulation can facilitate buckling [8] and crack propagation [9].

Active metals can improve the scale/metal adhesion and increase the behaviour during cycling by

different mechanisms, reducing voids formation at the interface, producing oxide pegs inside the matrix and modifying the plasticity of the scale.

As a consequence of the aforementioned mechanisms, some years ago AVESTA developed the grade 253MA (S30815) characterized by a nominal composition of 21% Cr, 11% Ni, 1.7% Si.

The aim of the present work is to compare the oxidation resistance of S30908, S31008, S30815 and of a new 22 Cr grade industrially produced by ILVA, called 309NC.

Experimental

The compositions of the investigated steels are given in Table 1. The S30908, S31008 and S30815 alloys are commercial products; the steel 309NC composition derives directly from S30908 as to Cr and Ni content while Mn was partly substituted by proper amounts of the austenitizing elements C+N. Si has been introduced at rather high levels (1.9%) and Ce was added in small amounts as mischmetal. The samples were cut from rolled and annealed sheets in the form of thin square specimens 20 mm × 20 mm × 3 mm. The surface preparation consisted of mechanical polishing up to 1 µm alumina paste, followed by ultrasonic degreasing.

The thermogravimetric tests have been performed in air, at constant temperatures, in the range 850 - 1150°C. The mass gain has been continuously recorded by a Cahn 1000 thermobalance (100 mg range, ± 0.2 mg). Unless differently stated, a mean curve specific mass gain vs. time has been reported; each test has been performed up to 330 hours or to 2 mg/cm². If such a mass gain is reached in a few hours the test is arrested.

The thermal cycling tests were carried out in air with 15 minutes holding time in the furnace and 5 minutes at ambient temperature. The specimens were weighted at regular intervals; the tests have been performed in the temperature range from 850 to 950°C, up to 3000 cycles (corresponding to 750 hours of holding time), unless a catastrophic oxidation occurred.

In order to get better insight into the scale morphology, compactness, thickness, adhesion, phases and elemental diffusion, the surface and metallographic cross sections were analysed by SEM and EDS apparatus.

TABLE 1 - Chemical composition of the alloys (wt%)

	S30908	S31008	S30815	309NC
Cr	22.4	25.5	21.3	22.9
Ni	14.5	19.2	10.8	13.4
Mo	0.18	0.20	0.24	0.13
Si	0.71	0.89	1.75	1.90
C	0.055	0.060	0.087	0.072
N	0.042	0.030	0.17	0.14
Ce	0.011	0.0024	0.035	0.041
Mn	1.68	1.10	0.49	0.42
S	0.0015	0.0033	< 0.001	< 0.001
P	0.033	0.016	0.016	0.018

Results

Isothermal tests:

In the Figures from 1 to 4 the experimental results of the isothermal tests are plotted as mass gain vs. time. The curves seem not to follow a parabolic rate law: therefore no rate constants have been calculated.

At the lower temperatures the expected shift of the curves with the temperature should be modified and a lesser mass gain with the rising of the temperature should happen because of a different chemical composition of the oxides which provides a better resistance. Sometimes different behaviours have been evidenced also at the same temperature, as for the S31008 (Fig. 2) and 309NC (Fig. 4) at 1050°C. At higher temperatures the mass gain is a balance between effective oxide formation and micro or macro-scaling, sublimation of CrO₃ or rupture and breakaway phenomena. Such a behaviour, which is typical of thermal cycling, is clearly shown in isothermal conditions at 1050°C for S30908 and 309NC steels and gives a bad repeatability of the tests.

Except for 900°C tests, the 309NC and S30815 alloys always behave better than the S30908 and S31008.

Cycling tests:

In the Figures from 5 to 8 the results of the cycling tests are reported. All the alloys show a final mass loss when cycled at or above 850°C, with the only exception of S31008 alloy which shows a not too large positive mass gain up to 900°C. For all the four alloys the highest test temperature resulted to be 950°C because of a general catastrophic oxidation.

Metallography:

Morphological features of the scales formed after isothermal and cycling oxidation tests at different temperatures are presented in Fig. 9-15.

Alloy S30908 - The scale formed in isothermal tests from 850 up to 1000°C consists of manganese-rich chromia microcrystals. The thickness of the outer layer increases with the temperature and easily spalls, leaving an inner silicon-rich layer (Fig. 9); this feature is common to the whole four alloys. At 1050°C and higher temperatures, manganese and iron-rich spinels appear. The X-rays maps on the cross sections show at the lower temperature (Fig. 10) a scale rich in Cr oxides, with an outer layer of Mn-rich spinels, discontinuous inner layers of silicon (or silicates) and an omogeneous matrix. The scale thickness rises with the rising of temperature, but a strong preferential oxidation along the grain boundaries and a decrease of chromium in the matrix occur. The silicon layer controls the Fe diffusion toward the scale: at 1050°C (Fig. 11) and at higher temperatures both Fe and Ni traces appear in the spinels, due to an imperfect local silicon control. The thermal stresses during cycling strongly modify the scale morphology. Continuous ruptures and local growths of the Cr-rich scale and of the Si-rich layer cannot allow the Fe control. Spalling occurs not only in presence of sudden mass losses, but also when the specimen seems to show a mass gain, as the process is governed by a balance between losses and gains.

Alloy S31008 - This steel is richer in Cr and poorer in Mn than the S30908. In isothermal conditions a thin chromia scale, with an outer layer of MnCr₂O₄ appears at 850°C; at higher temperatures the scales are often convoluted and contain interfacial cavities. The scales detach locally from the metal substrate thus reducing the high protectivity. At 950°C (Fig. 12) lateral oxide growth and buckling are evident, while at higher temperatures this phenomenon is less important. At 1000 and 1050°C the high diffusivity of all the elements doesn't allow the formation of a chromia scale and the oxide growth rates appear to increase. X-rays maps are similar to the already shown S30908 ones, except for local enrichments of Cr in the matrix at 850 and 900°C which suggests the formation of σ phase. In cycling conditions scale fractures and spalling are present. The analysis of a cross section (Fig. 13) reveals what is evident from the surface: a Cr healing occurs in correspondance to scale fracture thus controlling the mass growth.

309NC alloy - In isothermal tests the scale mainly consists of a thin chromium oxide with no growth

along the grain boundaries, possibly because of the rare earths effect. Spinel appears with the rising of the temperature. At 950°C (Fig. 14) the scale breakaway shows a spinel-rich outer layer, a silicon-rich layer and the substrate. At higher temperatures spinels are more and more important and the silicon layer, as revealed by the cross sections (Fig. 15), is no more continuous. Traces of the oxygen active elements Ce and La appear at the bottom of Si penetrations. The good healing capability of the matrix is evidenced in cycling oxidation tests.

Alloy S30815 - This alloy behaves in the same way of the 309NC.

Discussion

The mechanisms of scale growth control on such a grade of steels are mainly based on the selective chromium oxidation. The strongly protective Cr_2O_3 scale is weakened when, in presence of iron and manganese, tends to produce fast-growing mixed-spinel oxides. Iron spinels appear particularly dangerous. Silicon, whose oxygen affinity is similar to that of chromium, has a positive role in improving oxidation resistance. The enrichment at the metal/oxide interface in a silica-base layer, allows a reduction of diffusion through the scale of both Fe and Mn. Therefore, if Fe and Ni appear in the scale, the Si control is no more effective: this happens at the higher temperatures or during thermal cycling when mechanical stresses produce failures of the brittle silica-rich layer. The thickness of this layer appears a critical parameter of the scale protectiveness: a thick continuous layer easily controls the spinel formation, while a thin layer is tougher and better resistant to the thermal shocks. An optimum Si content of 0.6 - 1% is suggested in the literature [1].

Our results agree with this opinion as, in the case of isothermal oxidation, the best results are shown by the silicon rich 309NC and S30815 alloys. On the other hand, in the case of cycling oxidation, failures appear in the silica rich layer and the protection against the oxidation is guaranteed by the chromium healing capability against the spallation. The chromium rich S31008 alloy shows therefore the best performances in these severe conditions.

The oxide micrographies show a better control on oxidation with less convolutions in presence of Si and rare earths, thus confirming their strong and effective synergistic effect on scale composition and control reported in the literature [2].

Conclusions

Introducing an isothermal oxidation limit as the temperature corresponding to a steady state mass gain of 1 - 2 mg/cm^2 , the following ranking results from our experiences:

S30908, S31008	$T_{\text{max}} < 1000^\circ\text{C}$
309NC, S30815	$T_{\text{max}} < 1100^\circ\text{C}$

The highest temperatures in thermal cycling, with spallation and healing but before a catastrophic oxidation, appear to be:

S30908	$T_{\text{max}} < 850^\circ\text{C}$
309NC, S31008	$T_{\text{max}} \leq 900^\circ\text{C}$
S30815	$T_{\text{max}} = 850^\circ\text{C}$

The 309NC alloy results the most promising in both the test conditions; better performances should be attained reducing the silicon content at the 0.6-1% level.

References

- [1] Lobb R.C., J.A. Sasse and H.E. Evans. "Dependence of oxidation behaviour on silicon content of 20% Cr austenitic steels" Mater. Sci. Technol., 3 (1987), 828-834.
- [2] Bennett M.J., D.A. Desport and P.A. Labun. "Transverse microstructure of an oxide scale formed on a 20% Cr-25% Ni Nb stabilised stainless steel" Proc. R. Soc. A 412 (1987), 223-230.
- [3] Landkof M., A.V. Levy, D.H. Boone, R.G. Gray and E. Yaniv. "The effects of surface additives on the oxidation of Chromia-forming alloys" Corrosion, 41 (1985), 344-357.
- [4] Otsuka N., Y. Shida and H. Fujikawa. "Internal-external transition for the oxidation of Fe-Cr-Ni austenitic stainless steels in steam" Oxid. Metals., 32 (1989), 13-45.
- [5] Stott F.H. and F.I. Wei, "Comparison of the effects of small additions of Si or Al on the oxidation of Fe-Cr alloys" Oxid. Metals, 31 (1989), 369-391.
- [6] Wood G.C. and F.H. Stott. "Oxidation of alloys" Mater. Sci. Technol., 3 (1987), 519-530.
- [7] Stringer J., "Stress generation and relief in growing oxide films" Corr. Sci., 10 (1970), 513-543.
- [8] Srolovitz D.J. and M.P. Anderson "A criterion for compressive failure of a continuous protective surface film" Acta Metall., 32 (1984), 1089-1092.
- [9] Lowell C.E., J.L. Smialek and C.A. Barrett in "High temperature corrosion" Ed. R.A. Rapp, NACE Houston (1983), 291-226.

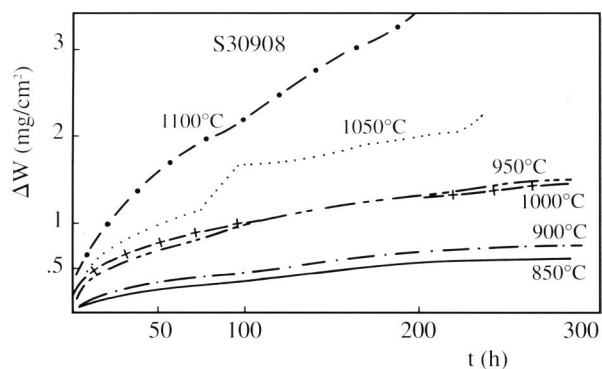


Fig. 1:

Mass gain/time curves for the S30908 steel in air isothermal tests at the indicated temperatures.

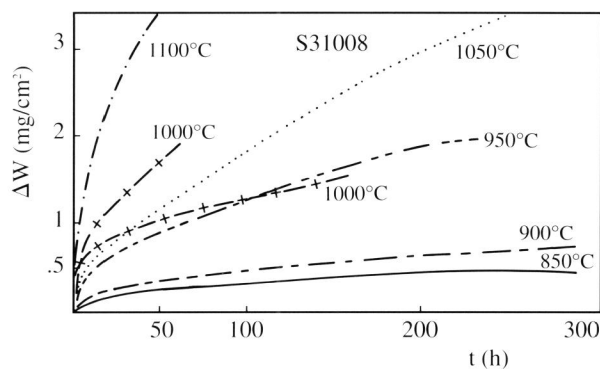


Fig. 2:

Mass gain/time curves for the S31008 steel in air isothermal tests at the indicated temperatures.

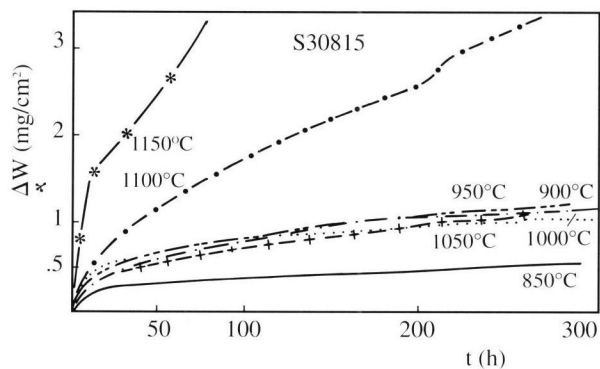


Fig. 3:
Mass gain/time curves for the S30815 steel in air isothermal tests at the indicated temperatures.

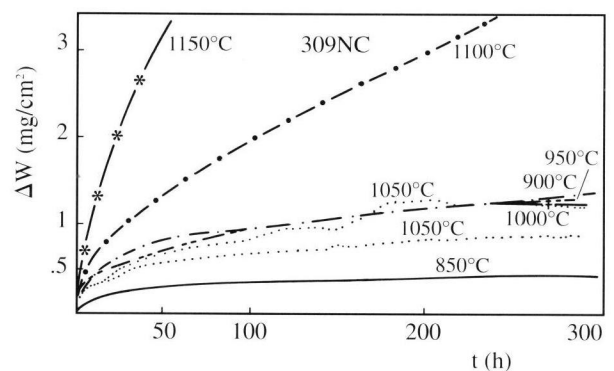


Fig. 4:
Mass gain/time curves for the 309NC steel in air isothermal tests at the indicated temperatures.

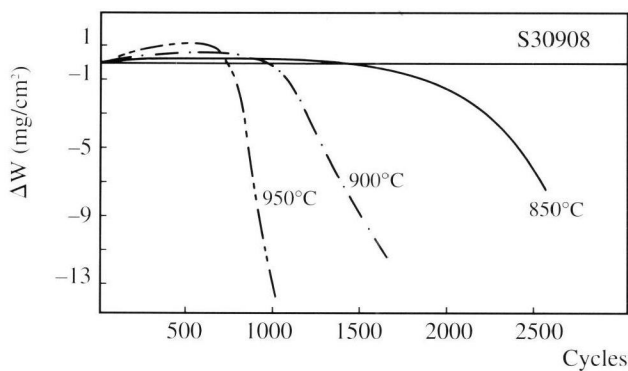


Fig. 5:
Mass gain/time curves for the S30908 steel in air thermal cycling tests (15 min at the indicated temperatures + 5 min at room temperature).

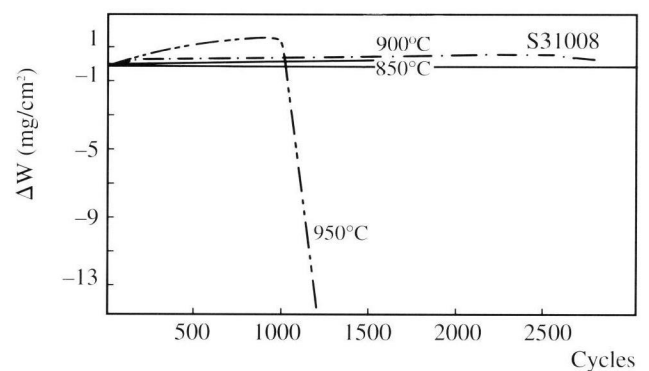


Fig. 6:
Mass gain/time curves for the S31008 steel in air thermal cycling tests (15 min at the indicated temperatures + 5 min at room temperature).

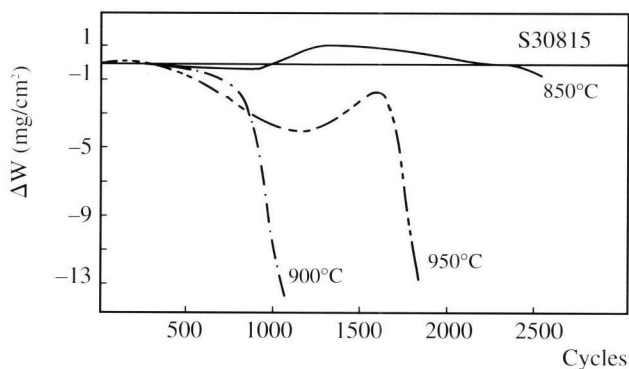


Fig. 7:
Mass gain/time curves for the S30815 steel in air thermal cycling tests (15 min at the indicated temperatures + 5 min at room temperature).

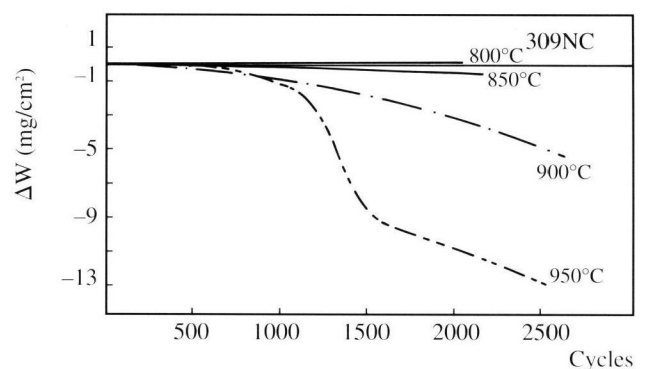


Fig. 8:
Mass gain/time curves for the 309NC steel in air thermal cycling tests (15 min at the indicated temperatures + 5 min at room temperature).

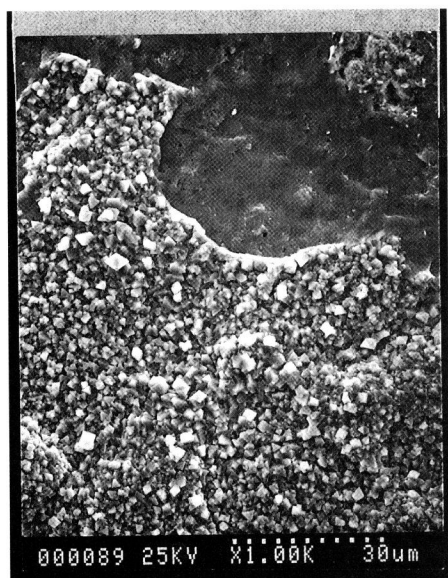


Fig. 9:
Morphology of the scale of the S30908 steel specimen after 300 h of isothermal oxidation in air at 900°C.

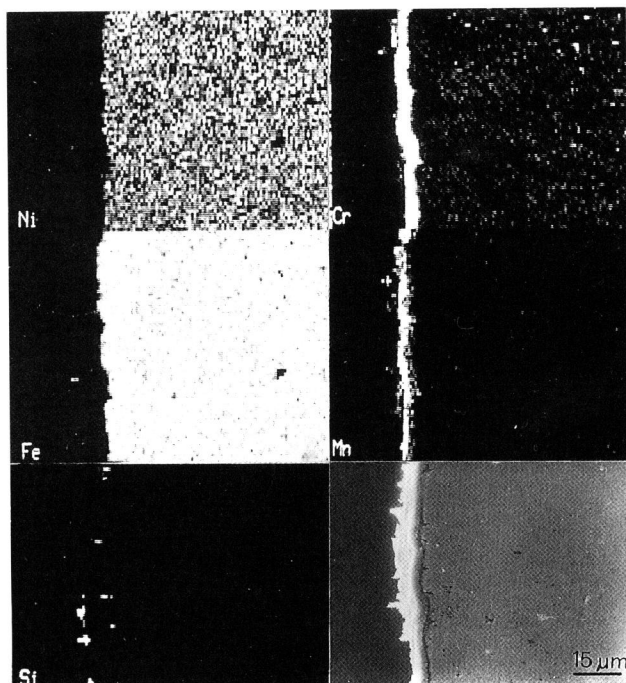


Fig. 10:
X-rays maps for Ni, Cr, Fe, Mn, Si on the cross section of the S30908 specimen isothermally oxidised at 850°C for 300 h.

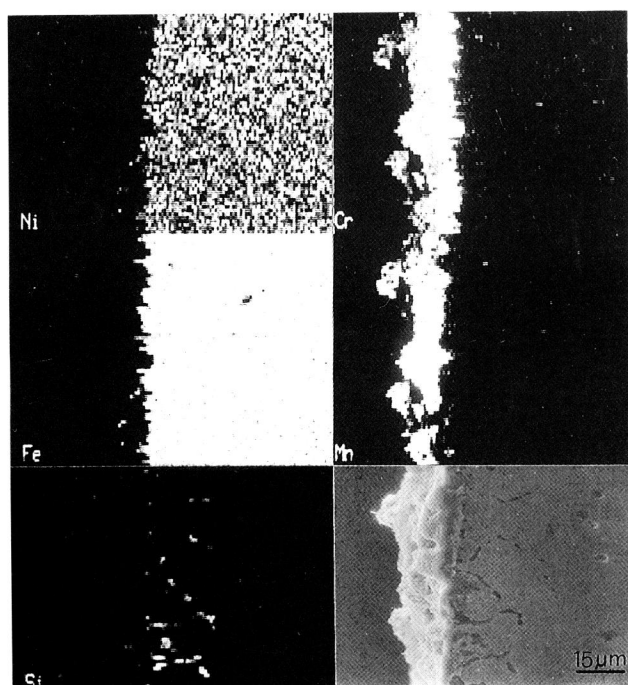


Fig. 11:
X-rays maps for Ni, Cr, Fe, Mn, Si on the cross section of the S30908 specimen isothermally oxidised at 1050°C for 250 h.

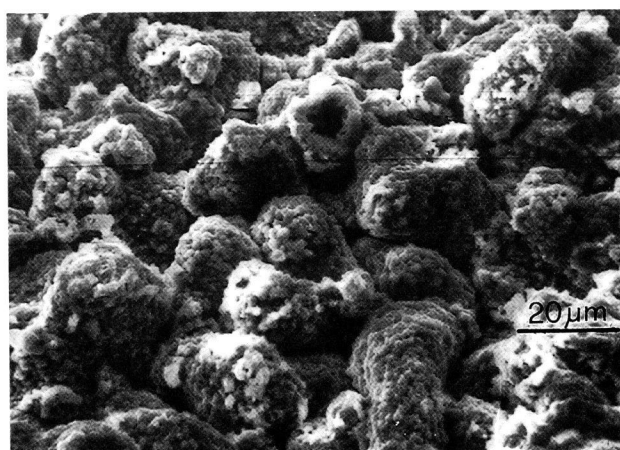


Fig. 12:
Morphology of the buckled scale for the S31008 steel isothermally tested in air 250 h at 950°C.

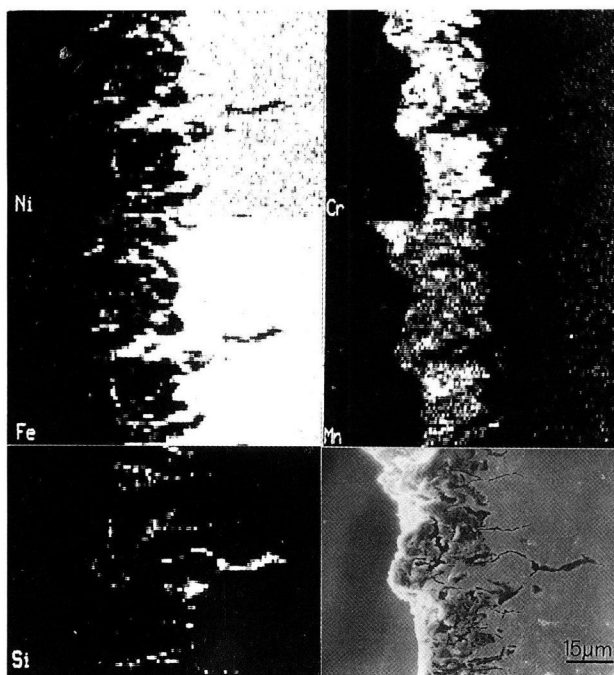


Fig. 13:
X-rays maps for Ni, Cr, Fe, Mn, Si on the cross
section of the S31008 specimen thermally cycled
in air at 950°C.



Fig. 14:
Scale morphology of a 309NC isothermally
oxidised in air 300 h at 950°C.

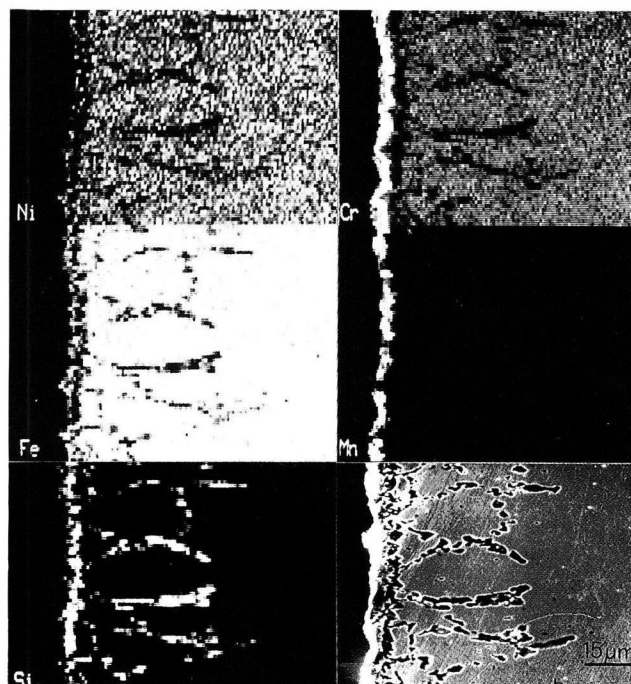


Fig. 15:
X-rays maps for Ni, Cr, Fe, Mn, Si on the cross
section of the 309NC specimen isothermally
oxidised at 1050°C for 300 h.